Vibronic Model Hamiltonian for the Study of the Near-IR−Visible Optical Properties of $[(NH_3)_5Ru-(4,4'\text{-bipyridine})-Ru(NH_3)_5]^{m+}$ ($m = 4, 5$): Charge Localization and Electroabsorption Spectra

Alessandro Ferretti,* Roberto Improta,† Alessandro Lami, and Giovanni Villani

Istituto di Chimica Quantistica ed Energetica Molecolare del CNR, Area della Ricerca, Via Alfieri 1, I-56010 Ghezzano (PI), Italy

Received: April 20, 2000; In Final Form: August 3, 2000

A vibronic model Hamiltonian suitable for the study of the optical properties in the near-IR−visible of partially localized systems is presented and discussed. The problem of how to deal with localization in a symmetric species is examined in view of understanding the origin of the observed Stark spectra. It is shown that a weak perturbation that breaks the symmetry of the Hamiltonian, such as that due to interaction with the solvent, allows charge localization in the ground state, as well as provides for a good prediction of the observed Stark spectra.

Introduction

Historically, mixed-valence chemistry begins in the 18th century, with the discovery of the Prussian and Turnbull Blue. However, modern aspects of mixed-valence chemistry, that is, those related to intramolecular electron delocalization, became of interest at the end of the 1960s, with the work of Robin and Day,[1] Hush,[2] and Creutz and Taube.[3] Robin and Day[1] have systematically classified mixed-valence materials into three classes, depending on the strength of metal−metal interaction. Hush,[2] besides a systematic review on the physical properties of known mixed valence compounds,[2a] made the first attempt to give them a theoretical interpretation.[2b] Finally, from the experimental side, Creutz and Taube synthesized the +5 pyz-bridged (pyz = pyrazine) Ru dimer and studied its optical properties in the near-IR−vis.[3] This compound, which is now the classic example of bridged mixed-valent metal dimer, gave rise to a strong debate aiming to understand whether or not its unpaired electron was localized on one of the two metals. The discussion has continued until Stark experiments by Oh, Sano, and Boxer[4] first, and then Raman measurements and crown ether encapsulation effects by Hupp and co-workers,[5,6] gave strong and clear indications that the system is delocalized (Ru(II.5)−Ru(II.5), instead of Ru(II)−Ru(III)). This is now also confirmed by DFT calculations.[7]

Since the Creutz−Taube work, a large variety of mixed valence compounds has been synthesized and studied, as shown in the review articles by Creutz,[8a] Crutchley,[8b] and Endicott and co-workers.[8c,d] Recent work to be cited is that by Olabe and co-workers[9] on Os-, Fe-, and Ru-bridged compounds, Crutchley and co-workers,[10] Meyer and co-workers,[11] and Endicott and co-workers.[12]

Theoretically, after the first paper by Hush,[2] several models have been proposed[13−21] in view of understanding and interpreting the observed near-IR−vis optical properties.

As far as the delocalized pyz-bridged Ru dimer is concerned, it is now well demonstrated that the essential physics involved in the properties related to the low energy states (those giving absorption in the near-IR−vis), can be ascribed to the combined effect of the Ru−pyz d−π* back-bonding interaction and electron correlation. The role of d−π* back-bonding interaction was first discussed by Ondrechen and co-workers in light of their local density (X_α) calculations.[14] The importance of correlation effects was later included by the formulation of a two-band Hubbard Hamiltonian,[17] which allows to reproduce and assign the observed spectra for the Ru dimer, as well as for its longer chain analogues,[22] as the total charge varies. The inclusion of selected nuclear degrees of freedom and vibronic coupling, which can also be investigated by DFT,[7] has made the model capable of reproducing the observed line-shape profile[18] as well as the Stark spectra[23] measured by Oh, Sano, and Boxer.[4]

On the other side, substituting pyz with 4,4′-bpy (bpy = bipyridine), one has a mixed-valence system whose Stark difference spectrum[4] is associated with a significant change of dipole moment during the transition, thus suggesting electron localization. In the visible, in the ∼2 eV region, a metal-to-ligand charge transfer (MLCT) transition is present for both the mixed-valent and the monovalent +4 species, as well as for the corresponding pyz compounds. At lower energy, a weak band is observed around 1 eV, which has been traditionally interpreted, in analogy with the pyz compounds, as due to an intervalence (IT) transition, i.e., to a metal-to-metal charge transfer (MMCT) between charge localized states with metallic character. The spectra of pyz and bpy species, however, show different behavior under the action of a static electric field for both the previously mentioned bands. Furthermore, the assignment of the 1 eV band in bpy compounds to an IT, although in accordance with the measured Stark spectrum, does not allow a straightforward explanation of the shift of the band toward higher frequencies with respect to that of the pyz compound. An extremely strong coupling with the solvent modes may be invoked to explain this effect, but then is not clear why the MLCT is almost unaffected.

Recently, a different assignment has been proposed by us,[21] grounded on a four-site model for bpy compounds, as a natural extension of the three-site one which is successful for pyz

* Corresponding author. E-mail: profin@ibm580.icqem.pi.cnr.it
† Present address: Dipartimento di Chimica, Università Federico II, Via Mezzocannone 4, I-80134 Napoli, Italy.

10.1021/jp0015168 CCC: $19.00
Published on Web 09/29/2000

compounds. Basically, we consider a π^* molecular orbital for each pyrazine ring. Our calculations with the Hubbard Hamiltonian show that, in contrast with the previous assignment, both the 1 and 2 eV transitions have a MLCT character. It is then worthwhile to examine in detail all the consequences of the model, in order to verify its capability of reproducing and interpreting experimental data.

In this article we move in this direction. While some new remarks on the four-site electronic model are given in the Appendix, the paper deals with the extension of the model to incorporate the effects of the coupling of electronic and nuclear motion. For the proposed vibronic Hamiltonian we will discuss the influence of the vibronic coupling on the absorption spectra and examine also the possibility that it may give rise to a symmetry breaking through charge localization in its ground state, with the crucial assistance of the solvent.

In this perspective, electroabsorption (EA) experiments (Stark),[4,24−27] i.e., the study of the effects of an external static electric field on the position and shape of the absorption bands can give valuable information on the electronic structure of mixed valence complexes, both in the ground and in the excited states, as well as on the extent of charge redistribution due to the optical transition, which translates into a measure of the change in the degree of localization of the unpaired electron.

Boxer and co-workers were the first to apply Stark spectroscopy to $(NH_3)_5Ru-pyz^{2+}$, $(NH_3)_5Ru-bpy^{2+}$, $[(NH_3)_5Ru]_2-pyz^{4+,5+}$, and $[(NH_3)_5Ru]_2-bpy^{4+,5+}$.[4] Their results have then been extensively analyzed by Hush and co-workers in terms of a two-state model.[28] Creutz et al. have then further examined the electroabsorption properties of $(NH_3)_5Ru-pyz^{2+}$, $(NH_3)_5Ru-bpy^{2+}$, and their protonated analogues.[27]

Experimental EA spectra can be analyzed in the terms of the Liptay theory,[24,29] in order to evaluate relevant physical quantities such as the transition moment, as well as the variation of electric dipole moment and polarizability associated with the electronic transition. These quantities can be related to the localized−delocalized nature of the mixed valence complexes.

We have then applied the vibronic model Hamiltonian to the study of absorption and electroabsorption spectra of a series of compounds, mainly in view of further investigate the validity of our model for partially localized compounds such as $[(NH_3)_5Ru]_2-bpy^{4+,5+}$. It is shown that the model, with a localized ground state and delocalized excited states, accounts for the observed EA spectra, although quantitatively a good agreement is difficult to be obtained.

The Four-Site Vibronic Model

The vibronic model for the species $[(NH_3)_5Ru-(4,4'\text{-bipyridine})-Ru(NH_3)_5]^{m+}$ ($m = 4, 5$) that we want to study is built in analogy to that for the pyz compounds of ref 23b. We proceed in two steps, considering first the purely electronic Hamiltonian and then including nuclear degrees of freedom and vibronic couplings. This section is thus divided into two subsections: the electronic model and the vibronic model.

The Electronic Model. The electronic part is that extensively discussed in ref 21 in which only one d orbital for each Ru atom (the d_{xz} for the pyr ring in the *yz* axis with $Ru-N_{pyr}$ on *z*) and one π^* for each pyr ring of bpy have been taken, so that the bpy compounds are seen as a M−L−L−M system. This picture allows to properly consider the effects of Ru−pyr back-bonding interaction and electron correlation, which play the most important role in determining the observed properties of the states at low energy. We can then write the Hubbard Hamiltonian,[30] of the partially localized system (H_{pl}) for electrons:[21]

$$H_{pl} = \sum_{\sigma}[\Delta(n_{2,\sigma} + n_{3,\sigma}) + t(a^+_{1,\sigma}a_{2,\sigma} + a^+_{3,\sigma}a_{4,\sigma} + \text{hc}) + t'(a^+_{2,\sigma}a_{3,\sigma} + \text{hc})] + U\sum_{j}^{\text{Msite}} n_{j,\uparrow}n_{j,\downarrow} + U_L\sum_{j}^{\text{Lsite}} n_{j,\uparrow}n_{j,\downarrow} \quad (1)$$

where $a^+_{j\sigma}$ ($a_{j\sigma}$) is the creation (annihilation) operator for one electron with spin σ in the orbital of site j, $n_{j\sigma} = a^+_{j\sigma}a_{j\sigma}$, $\Delta = \epsilon_{pyr} - \epsilon_{Ru}$. t and t' are metal−ligand and ligand−ligand resonance integrals (or hopping), respectively. U and U_L are the Coulomb repulsion terms, respectively, for Ru and for pyr π^*. Metal sites are 1 and 4, and ligand sites 2 and 3. The vacuum is Ru(IV).

In the Appendix we show that, according to the 4-site model, the 1 eV and 2 eV bands are both derived from MLCT transitions present in the monometallic species.

The Vibronic Model. Relevant nuclear degrees of freedom for the compounds in study are certainly the vibrations localized respectively on the $Ru(NH_3)_5$ and pyr moieties (site vibrations),[13,15−20,23] which have already been utilized in the study of the line-shape profile[18] and electroabsorption spectra[23] for the pyz-bridged Ru dimer. However, since near-IR−vis optical properties and electroabsorption spectra are polarized along the Ru−Ru (*z*) axis, it has to be expected that these are also affected by the change of Ru−pyr and pyr−pyr bond lengths.[20] Therefore, we want also to take into account the bond vibrations. This can be done taking one harmonic oscillator to model each local vibration, site, and bond, and we have thus the following vibrational model Hamiltonian:

$$H_v = \sum_{j}^{\text{Nsite}} \omega_j\left(b^+_j b_j + \frac{1}{2}\right) + \sum_{j}^{\text{Nsite}-1} \omega_{j,j+1}\left(b^+_{j,j+1}b_{j,j+1} + \frac{1}{2}\right) + \sum_{j}^{\text{Nbond}-1} \frac{1}{m_{pyr}}p_j p_{j+1}$$

$$p_j = i(b^+_{j,j+1} - b_{j,j+1})\sqrt{\frac{\mu_{j,j+1}\omega_{j,j+1}}{2}} \quad (2)$$

where b^+_j (b_j) and $b^+_{j,j+1}$ ($b_{j,j+1}$) are the creation (annihilation) operators for one-quantum excitation, respectively in the site oscillator j with frequency ω_j and in the bond oscillator between sites j and $j + 1$ with frequency $\omega_{j,j+1}$ ($\hbar = 1$), m_{pyr} is the reduced mass of one pyridine ring and $\mu_{j,j+1}$ is the reduced mass of the jth bond (that between sites j and $j + 1$). The last term of eq 6, which involves the momenta p_j of the j,$j + 1$th bond oscillator, is the kinetic coupling term arising from the transformation of the kinetic energy matrix in the local bond basis, where it is no more diagonal.[31]

The total molecular Hamiltonian (H_{mol}) is then obtained including the proper vibronic coupling term (H_{el-v}):

$$H_{mol} = H_{el} + H_v + H_{el-v}$$

$$H_{el-v} = \sum_{j,\sigma}^{\text{Nsite}} \lambda_j n_{j,\sigma}(b^+_j + b_j) + \sum_{j,\sigma}^{\text{Nsite}-1} \gamma_{j,j+1}(a^+_{j,\sigma}a_{j+1,\sigma} + \text{hc})(b^+_{j,j+1} + b_{j,j+1}) \quad (3)$$

where H_{el} is the electronic Hamiltonian for the partially localized system of eq 1, H_{pl}. The two terms in H_{el-v} represent the vibronic coupling for site and bond oscillators which can be derived, respectively, by expanding the site energy (ϵ) and the

resonance integral (t) on the corresponding nuclear coordinate. The first term, that for the site oscillators, is associated with a displacement of the equilibrium position when the corresponding orbital is populated. The second, which was first introduced in a different context by Bozio and co-workers,[32] is associated with a displacement of the bond oscillator when the electron hops between the two sites forming the bond.

When the molecule is embedded in static electric field, the total field-molecule Hamiltonian results:

$$H = H_{\mathrm{mol}} - \mu E \tag{4}$$

where E is the electric field and μ the dipole operator. This latter, which depends on the bond coordinates s, may be derived by the transformation:

$$s = \begin{pmatrix} -1 & 1 & & \\ & -1 & 1 & \\ & & -1 & 1 \\ \frac{m_1}{M} & \frac{m_2}{M} & \frac{m_2}{M} & \frac{m_1}{M} \end{pmatrix} x \tag{5}$$

where x are the Cartesian coordinates of the four sites, m_1 and m_2 the mass of the $Ru(NH_3)_5$ and pyr fragments, respectively, and M is the total mass of the molecule. The s_4 coordinate is that of the center of mass, and we center the reference in this point so to have that a centrosymmetric charged species has zero dipole moment.

The form of the dipole operator then follows:

$$\mu = \sum_{i}^{\mathrm{Nsite}} n_i \langle i|x|i\rangle = \sum_{k}^{3} \bar{\mu}_k$$

$$\bar{\mu} = \begin{pmatrix} -\frac{(m_1+2m_2)s_1}{M} & \frac{m_1 s_1}{M} & \frac{m_1 s_1}{M} & \frac{m_1 s_1}{M} \\ -\frac{s_2}{2} & -\frac{s_2}{2} & +\frac{s_2}{2} & +\frac{s_2}{2} \\ -\frac{m_1 s_3}{M} & -\frac{m_1 s_3}{M} & -\frac{m_1 s_3}{M} & \frac{(m_1+2m_2)s_3}{M} \end{pmatrix} \begin{pmatrix} n_1 \\ n_2 \\ n_3 \\ n_4 \end{pmatrix} \tag{6}$$

where n_i is the number of electrons in the site i.

Since the EA spectra are measured in a glassy matrix where the molecules are randomly oriented with respect to the static field, it is necessary to perform an average over the orientations ($\langle S \rangle$). As shown in ref 23b (eqs 5−8), this can be accomplished by the equation

$$\langle S \rangle = K \int_0^{\pi} S_\theta \sin^3 \theta \, \mathrm{d}\theta \tag{7}$$

where we have taken the angle between the static field E and the exciting field to be 90°, θ is the angle between E and the molecular axis z (Ru-pyr-pyr-Ru axis), S_θ is the spectrum computed at a given value of θ, and K is a constant (see eq 8 of ref 23b) whose value is not relevant for the present purposes (the intensities of the bands are scaled so to have a computed zero-field spectrum normalized to the experimental one; see also ref 23b).

The values of the parameters for the electronic Hamiltonian are those discussed and utilized in previous papers,[21] that is (in eV):

$$t = -0.73, \quad t' = -0.15, \quad \Delta = 5.06, \quad U = 4.62 \quad U_{\mathrm{L}} = 2.5$$

For the parameters of the site oscillators, in line with previous studies,[15,18,23] we have considered on each $Ru(NH_3)_5$ moiety one oscillator with the frequency of the $Ru-NH_3$ symmetric stretch of $Ru(NH_3)_6$ ($\omega = 500$ cm^{-1}), and one oscillator with the frequency of the symmetric ν_{6a} mode of pyrazine for each pyr ring ($\omega = 609$ cm^{-1}). The corresponding values of the vibronic coupling parameters (λ's in eq 3) are −0.1 and −0.16 eV, respectively for the Ru site (λ_1 and λ_4) and for the pyr site (λ_2 and λ_3).[15,18,23]

For the bond oscillators, frequencies and vibronic parameters have been estimated from the Raman resonance spectra of the 4,4′-bpy and pyz compounds by Hupp and co-workers.[5,33] The authors find that the pyr−pyr stretch is at $\omega_{2,3} \sim 1300$ cm^{-1} and that Ru−N (N of the organic ligand) symmetric stretch is at 328 and 391 cm^{-1}, respectively, for pyz and bpy.[33,34] From these values one can estimate a frequency around 600 cm^{-1} for the local bond vibrations ($\omega_{1,2} = \omega_{3,4}$ for bpy), which seems too high considering the mass of the ligand. We have then assumed that the 328 and 391 cm^{-1} frequencies are those of the local bond stretch. A later study of the pyz Ru dimer by DFT [7] has reported the local bond vibration at ∼250 cm^{-1}, and with that value our results does not change significantly.

Since for the pyz compounds the adimensional displacement between the equilibrium Ru−N distance ($\Delta r_{1,2}$) is predicted to be 1.26, it is possible to derive the value of $\gamma_{\mathrm{Ru-pyz}}$ through the relation[5b]

$$\gamma_{1,2} = \gamma_{3,4} = \frac{\mu_{1,2}\omega_{1,2}^{\,2}\Delta r_{1,2}}{\sqrt{2\mu_{1,2}\omega_{1,2}}} \tag{8}$$

which gives $\gamma_{\mathrm{Ru-pyz}} = 0.021$ eV.

For the bpy Ru dimer there is no experimental evidence for the values of $\Delta r_{1,2}$, as well as of $\Delta r_{2,3}$ (the displacement of pyr−pyr mode) and it is not easy to estimate the values of γ's. However, since we do not expect a large difference between bpy and pyz Ru−N stretch, for $\gamma_{1,2} = \gamma_{3,4}$, we have explored the range 0.025−0.07 eV, close to the value of $\gamma_{\mathrm{Ru-pyz}}$.The results shown are those for $\gamma_{1,2} = \gamma_{3,4} = 0.05$ eV.

As far as the pyr−pyr vibronic coupling $\gamma_{2,3}$ is concerned, taking into account that when 4,4′-bpy acquires an electron[35] the pyr−pyr bond distance decreases by ∼0.1 Å, and that our electronic model calculations predict that near-IR−vis transitions involve a partial MLCT (∼0.3 electrons), we can estimate that $\Delta r_{2,3}$ is reasonably in the range 0.01−0.02 Å. An application of eq 4 yields the value of $\gamma_{2,3}$ in the range −0.04−0.08 eV. In our calculation we have used a value of −0.06 eV, and we have verified that the results are not significantly changed by small variations of this value.

Charge Localization

We want to discuss now charge localization, as seen in the framework of our approach.

It is conceptually useful to begin considering the ion as an isolated entity, which can be described, for example, by the vibronic model Hamiltonian of eq 3. This must then retain the full symmetry of the problem and the consequence is that all eigenstates will result in being completely delocalized. We are then faced with the problem of how to see the tendency toward charge localization, since it is clear that the Hamiltonian for the system does not allow symmetry breaking.

In the framework of the adiabatic approximation we can give an answer. In fact, a system approaching the localized limit in a given electronic state (for example the ground) will show a double well in the space of nuclear coordinates. Furthermore, a

wave packet localized in one of the two minima should require a sufficiently long time to overcome the barrier and reach the other minimum. It is therefore possible to find the mixed-valent ion in a definite charge-localized state (this then gives rise to the problem of the preparation of the system in a nonstationary state). In some cases the time for electron transfer may become so long that the two charge-localized states may be considered, with a good approximation, as stationary.

However, our approach to the problem consists of finding the exact ground state through a numerical iterative (Lanczos) procedure. Thus we always converge to a delocalized ground state (eigenstate of H), which is the lowest combination of the two localized states. The sign of localization is then given by the existence of a nearly degenerate state with opposite symmetry (the other combination of localized states). Thus, for example, if the ground state is symmetric with respect to the inversion center, the near-degenerate state will be antisymmetric and their combination will give a pair of (weakly interacting) charge localized states. These two states are those giving rise to the IT transition, and smaller its energy and intensity, the higher its tendency toward localization.

To overcome the problem of convergence to a delocalized state, we can use in practice a simple trick; i.e., we introduce a small asymmetry in the Hamiltonian. If the system is in a situation like that described above (almost degenerate ground state), then such a small perturbation, which can be the interaction with the solvent, is sufficient to give rise to a true localized ground state. Therefore, while it is in principle possible that particular mixed-valent ions can be observed in a charge-separated state, i.e., in a nonstationary state, in conditions where they can be considered as isolated (i.e., in an hypothetical beam or in a gas-phase experiment at low pressure), in general the role of the interaction with the solvent is expected to be crucial. In fact, the introduction in the model Hamiltonian of the manifold of solvent and internal modes coupled with the electronic motion, increasing the electron-transfer time, is in favor of charge localization.

It is important to stress that even when the charge-localized ground state is quasi-stationary, one is, in principle, not allowed to work with a symmetry-broken Hamiltonian: the system may still be delocalized in the excited states.

When we consider the role of a slowly relaxing solvent surrounding the mixed-valent ion, as in the Stark experiments, usually performed in a glassy water−glycerol matrix at 77 K, we have a conceptually different situation. Now, the rearrangement of the solvent nuclear degrees of freedom accompanying the charge motion may become so slow that can be neglected. In such a case, a species that, when isolated, exhibits a marked tendency toward localization in its ground state will certainly give rise to a charge localized state, with the solute surrounded by solvent molecules that minimize the total energy. Since we now can neglect solvent reorganization (very slow), solvent acts introducing a real symmetry breaking in the Hamiltonian, under the form of a finite perturbation that stabilizes one of the charge separated forms.

The above discussion on localization is not simply academic. As discussed in the following, the Stark spectra of a given species may look quite different, depending on whether the charge is or not localized in the ground state. On the other hand, the absorption spectra are insensitive of localization. In fact, since in a Stark experiment on these compounds the only active component of the external field is that along the molecular axis, an average over all possible molecular orientation[23b] must be performed. Then, if a species is localized in the ground state,

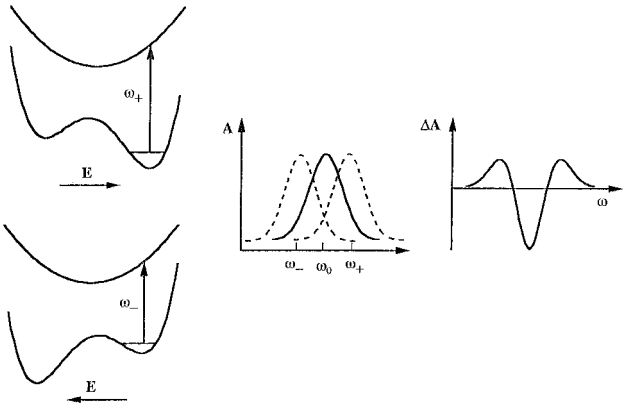

Figure 1. A system with charge localization in the ground state can be schematized in one dimension (the molecular axis) by a symmetric double well. This symmetry, in a Stark experiment, is removed by the component (+ or −) of the external electric field along the molecule. The two potential curves on the left of the figure are thus obtained, which give rise to two displaced bands (dashed line) on the two opposite side of the zero-field spectrum (continuous line). The resulting difference spectrum (ΔA; to the right) has thus the positive−negative−positive shape observed in the experiment.

and the energy barrier between the two charge-localized states is much larger than the energy gap induced by the field, one has, according to the scheme of Figure 1, a Stark spectrum as that observed experimentally for partially localized bpy compounds.

The applied electric field may be effective in inducing charge localization in some isolated systems, since it plays exactly the role of introducing a small asymmetry in the Hamiltonian (which becomes then a real perturbation and not a numerical trick for unravelling the tendency toward localization, as discussed before). However, this field-induced localization is not what is needed for explaining the behavior of Stark spectra in localized systems. In fact, it would give rise to a strongly polarized (in the direction of the field) ensemble of charge-localized molecules, whereas the output of Stark spectra on such systems can be easily interpreted assuming that the way a given species is charge-localized (i.e., the direction of its dipole) is independent of the direction of the applied electric field. In our investigation on the charge localization and Stark spectra we have then introduced a solvent-induced asymmetric perturbation which is dominant on the one induced by the applied electric field.

The vibronic model Hamiltonian of eq 3 takes into account "exactly" the interplay between electron and nuclear motion, from both the static and dynamic point of view. When confronting the results obtained with the full vibronic Hamiltonian with those obtained with the electronic Hamiltonian of eq 1, we may use expressions like "vibronic induced effect", simply meaning an effect that can be generically ascribed to the coupling of the motion of electron and nuclei.

We notice that some confusion exists in the present terminology, and it may be useful to make it clear here that the term "vibronic" is not used by us as a synonym of "due to nonadiabatic coupling" or " due to the breakdown of the BO approximation". In fact, when we move from the electronic Hamiltonian to the full vibronic one, we make two steps forward, going directly from a limit where any dependence on nuclear coordinates is disregarded, to that in which both adiabatic effects (due to the introduction of a dependence of the Hubbard parameters on nuclear coordinates) and nonadiabatic effects (due to the nuclear kinetic energy operator) play a role. It may not be always clear (at least without further investigation) if what we find, passing from one limit to the

other, can be simply explained within the adiabatic approximation, or nonadiabatic couplings must be invoked. The term "vibronic" allow us to maintain this ambiguity.

As previously discussed, there is a number of vibrational coordinates that may play a significant role in promoting localization through vibronic effects. In the present paper we have investigated the following: the bond stretching between adjacent sites (s_{12}, s_{23}, s_{34}) and an intrasite oscillator for each site (x_1, x_2, x_3, x_4). In the case of the Ru sites (x_1, x_4) these represent a symmetric stretching in which all the Ru−NH_3 bonds are involved, while in the case of the pyridine sites (x_2, x_3) these are symmetric ring stretches involving C−C and C−N. The intrasite coordinates concern degrees of freedom that are not directly involved in the bonds formed by the orbitals included in our model Hamiltonian. They play, however, an indirect role, modulating the site energies.

In the following we will present the results obtained by two different approaches: adiabatic, i.e., obtained diagonalizing the 24 × 24 matrix at various nuclear configurations, and exact, i.e., by a numerical diagonalization of the vibronic Hamiltonian. This way of proceeding is not only a necessity, since one cannot perform exact calculations involving all the modes, but also useful since the adiabatic calculations can furnish a more general picture.

1. Adiabatic Results. We have studied the adiabatic surfaces as a function of all the previously introduced degrees of freedom, i.e., the three intersite stretchings and the four intrasite coordinates. We have simply to neglect the momenta in eq 3, choose a point in our seven-dimensional nuclear space, and then diagonalize the resulting 24 × 24 electronic matrix. We find convenient to introduce symmetric and antisymmetric combinations of coordinates: s_{23}, $x = s_{12} + s_{34}$, $y = s_{12} - s_{34}$, $u = x_{11} + x_{44}$, $v = x_{11} - x_{44}$, $w = x_{22} + x_{33}$, $z = x_{22} - x_{33}$. The diagonalization gives a point in the eight-dimensional energy-coordinates space for each adiabatic electronic surface.

Let us focus first on the ground state. Adopting a numerical gradient method, we have found that there is a single minimum along all the symmetric and a double minimum along the antisymmetric coordinates. The section along the *z* coordinate is, however, quite flat and we have then focused on the (y,v) plane, that of the antisymmetric combinations of the two Ru intrasite oscillators (y), and of the two Ru−pyr bond oscillators (v). The ground state in the (y,v) plane is shown in Figure 2. The vibronically induced localization can be clearly seen under the form of a double-minimum potential energy surface.

The two minima, as expected, are symmetrically placed with respect to the origin, at ($y = -0.092$ Å, $v = 0.160$ Å) and ($y = 0.092$ Å, $v = -0.160$ Å), and separated by a potential energy barrier of about 539 cm^{-1} (as measured along the straight path). It is interesting to notice that, according to our choice of parameters, the two Ru−pyr bond oscillators are the more effective in promoting localization, as demonstrated from the fact that the line connecting the two minima forms a smaller angle with the v axis (∼30°) than with the *y* axis (∼60°).

As far as the MLCT excited states are concerned, whose potential energy surfaces are not reported for the lack of space, these are found to have a single minimum. This clearly indicates that, although the ground state can be localized, the excited MLCT's are delocalized.

Solving the vibrational problem on the surface in Figure 2, we obtain a delocalized ground vibrational state, which is, however, separated by only 1.4 cm^{-1} from the first excited state (exhibiting the opposite symmetry with respect to reflection).

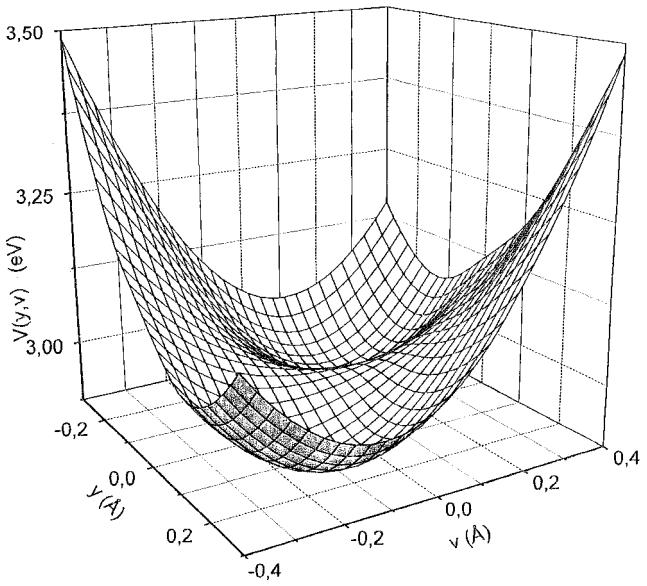

Figure 2. Adiabatic potential energy surface for the ground state along the two asymmetric coordinates *y* and *v* (see text for definition).

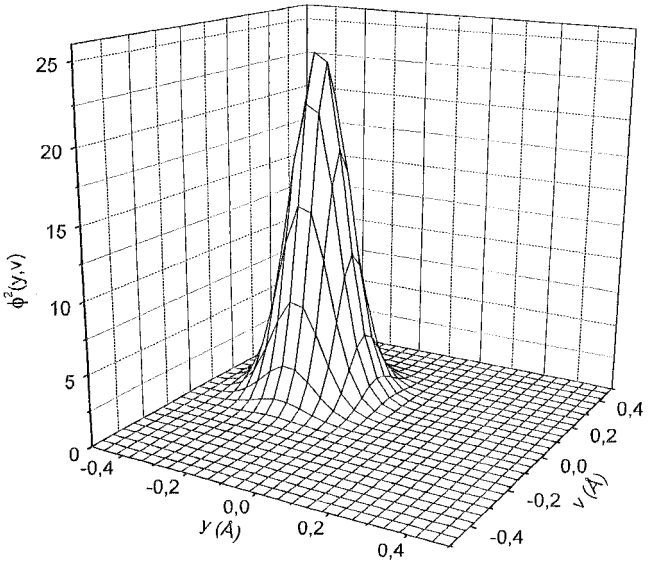

Figure 3. Localized ground-state wave packet as obtained by the PES of Figure 2 introducing an asymmetrization of 100 cm^{-1} in the Hamiltonian.

This means that according to the adiabatic picture, a wave packet localized in one well takes about 12 ps to reach the other well, in the isolated ion.

We can mimic a situation in which the charge-localized configuration is stabilized by solvent coupling by a hundred cm^{-1} (while the solvent relaxation, as discussed, is so slow that it can be neglected), introducing a symmetry-breaking term in the Hamiltonian.

Figure 3 shows the vibrational ground state obtained assuming that both the right sites (Ru and pyr ring) are stabilized by 100 cm^{-1}; it is clear that this is largely sufficient to give rise to a true localized ground state.

2. Exact Calculations. As previously mentioned, the exact calculations including the same seven oscillators as in the adiabatic calculations are computationally not affordable (several tens of millions of states are required). For this reason we have decided to perform two distinct studies, one involving the intrasite oscillators and the other the three bond oscillators (two Ru−pyr and one pyr−pyr).

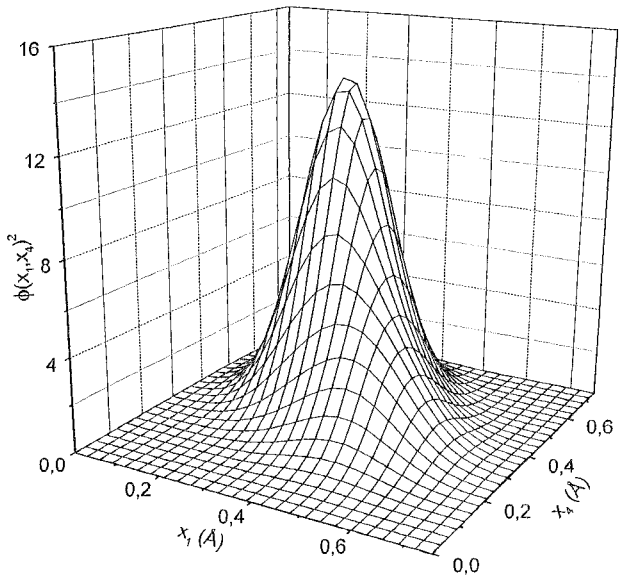

Figure 4. Ground state wave packet by exact vibronic calculations which only take into account site oscillators. An asymmetry of 5 cm^{-1} in the Hamiltonian has been added. The state is delocalized.

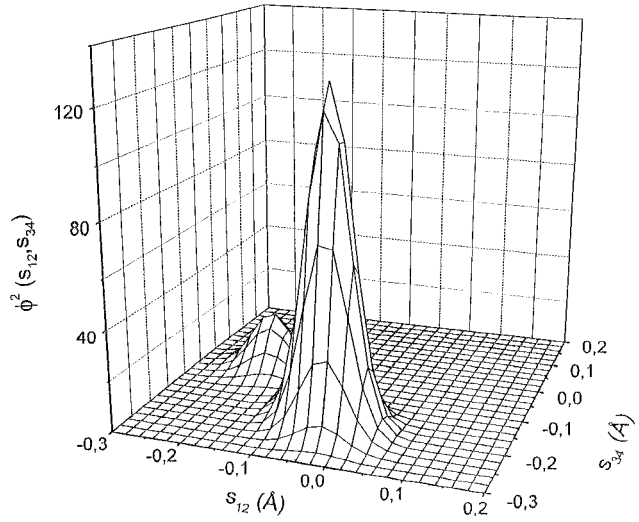

Figure 5. Localized ground state wave packet by exact vibronic calculations which only take into account bond oscillators. An asymmetry of 5 cm^{-1} in the Hamiltonian has been added.

The computational method, which has been described in detail elsewhere,[18] involves the use of a basis built as tensorial product of localized electronic states and harmonic oscillator states and the use of an iterative Lanczos algorithm to generate the ground state, starting from a trial vector.

Figures4 and 5 show the ground state wave packet for the case including only the two intrasite oscillators (mimicking a pseudosymmetric expansion/contraction of the coordination sphere on the Ruthenium sites), and for the case considering the three bond oscillators, respectively. Here we have introduced from the beginning a symmetry-broken Hamiltonian, which takes into account the solvent effect described previously. In practice, as in the adiabatic calculation, we have lowered the site energies for both the right Ru and pyr sites by the same quantity, 5 cm^{-1}. Figure 4 clearly shows that the intrasite oscillators are not very effective in localizing, as predicted by the adiabatic calculation. In fact, the wave packet is strongly asymmetric but not completely localized. The vibronic effect of the bond oscillators (Figure 5) is instead sufficient to give rise to complete localization and the asymmetry required for

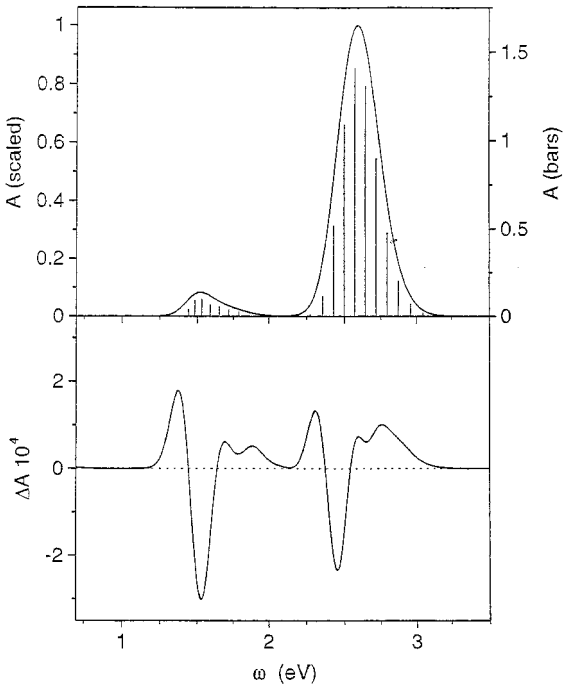

Figure 6. Absorption (upper part) and electroabsorption (lower part) spectrum of $[(NH_3)_5Ru-(4,4'\text{-bpy})-(NH_3)_5Ru]^{5+}$ as computed including only bond oscillators.

charge localization is now (5 cm^{-1}) much smaller than in the adiabatic calculations (100 cm^{-1}) of the previous section.

Absorption and Electroabsorption (Stark) Spectra

1. $(NH_3)_5$Ru-pyr-pyr-Ru$(NH_3)_5^{5+}$. In the previous section, we have shown and discussed how the ground state of this species can be localized, differently from the excited states. Indeed, the calculation of EA spectrum performed without any asymmetry in the Hamiltonian is not in agreement with the experimental results: whereas the band at ~2 eV in the visible has a second derivative character, the computed shape of the band at ~1 eV only shows a first derivative component, with a negative lobe followed by a positive one. However, the computed absorption spectrum is instead in agreement with the experimental one and is about the same of that obtained introducing the asymmetry in the Hamiltonian (upper part of Figures 6 and 7), since with no external field the two minima of the PES are degenerate. According to the electronic model Hamiltonian of ref 21, on which our vibronic model is based, the two bands at ~1 and ~2 eV are both MLCT.

As already discussed, our full vibronic calculations cannot give directly the localized ground state, this is then built by the linear combination of the nearly degenerate symmetric and the antisymmetric delocalized states. The spectra are then obtained propagating the localized ground state with the full Hamiltonian, in absence and in the presence of the field.

Since, as previously discussed, the complete full vibronic calculation is too heavy, we have performed only calculations with the bond oscillators (Figure 6) and the site oscillators (Figure 7) separately. The vibronic basis set for bond oscillators is made by 21 states on the Ru−pyr oscillator and 11 on that pyr−pyr (for a total vibronic basis of 116 424 states). In the case with site oscillators alone, the vibrational basis set is made by 12 states on Ru and 5 on pyr sites (for a total vibronic basis of 86 400 states).

In both cases (upper part of Figures 6 and 7), the absorption spectrum is rather similar to the experimental one,[4] with a broad

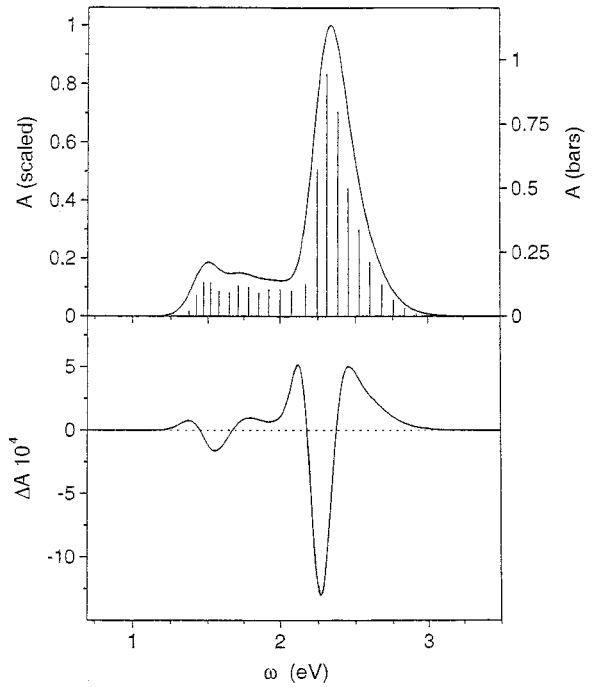

Figure 7. Absorption (upper part) and electroabsorption (lower part) spectrum of $[(NH_3)_5Ru-(4,4'\text{-bpy})-(NH_3)_5Ru]^{5+}$ as computed including only site oscillators.

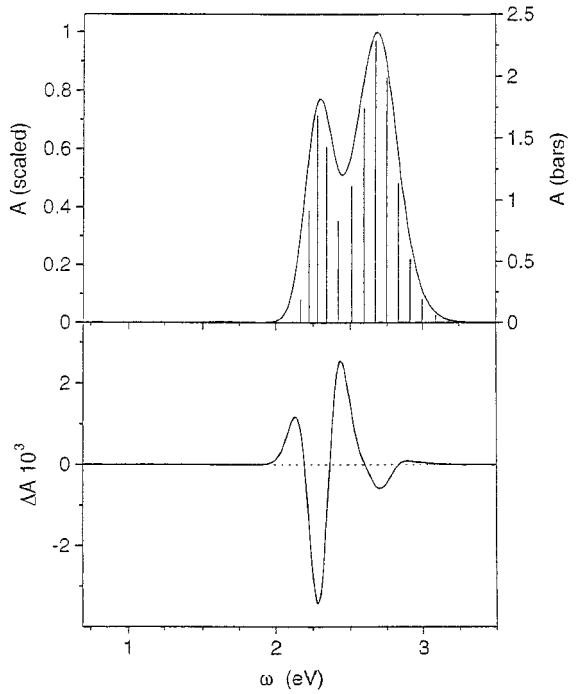

Figure 8. Absorption (upper part) and electroabsorption (lower part) spectrum of $[(NH_3)_5Ru-(4,4'\text{-bpy})-(NH_3)_5Ru]^{4+}$ as computed including only bond oscillators.

and weak band at ~1.4 eV and a sharp and much more intense peak at ~2.5 eV. There is still present a very weak band centered at ~0.1 eV, reminiscent of the symmetric−antisymmetric transition occurring in the delocalized calculations; however, some test calculations performed using a vibronic constant for the Ru−pyz stretch of 0.07 eV shows that the intensity of that peak goes rapidly to zero.

The EA spectra (lower part of Figures 6 and 7) show that both cases are characterized by bands having large second derivative contribution, in agreement with the analysis of the experimental EA spectrum performed following the Liptay theory.[4] In the experimental EA spectra the highest energy positive lobe of the first band is seen to merge with the first positive lobe of the second. This can be due to the effect of nuclear degrees of freedom, such as the torsion of the two rings, that have not been included in the model, as well as to the fact that we have considered bond and site oscillators only in separate calculations. In fact, in the calculations with the site oscillators of Figure 7 (vibronic coupling constants taken from ref 18) the bands in the IR and in the visible indeed start merging (Figure 7), but in this case the EA spectrum has the feature at ~2 eV much more intense than that at ~1 eV, which does not happen with bond oscillators. This strongly suggests that the agreement with the experimental EA spectra can be improved by the simultaneous inclusion of bond and site oscillators.

In the present case, we have added a symmetry breaking term in the Hamiltonian which allows localization in the ground state, while for the propagation of the doorway state ($\mu|g\rangle$) we use the true (symmetric) Hamiltonian, with the justification that according to the adiabatic calculations of the previous section, the excited states do not exhibit any localization effect. If our scheme is valid, then the excited MLCT states will have zero dipole moment (they are delocalized), while the localized ground state has a dipole moment (computed) of 16.1 D. This value is close to the 21.4 D evaluated experimentally in ref 4b and is much smaller than the 54.3 D expected for the transfer of one electron. The reason for this difference is that the net charge-transfer accompanying excitation involves less than one electron, since in the ground state the ligand orbital is already populated.

2. $(NH_3)_5Ru\text{-pyr-pyr-}Ru(NH_3)_5^{4+}$. The spectrum obtained including only the bond oscillators (21 states on Ru−pyr oscillators, 11 on pyr−pyr oscillator, for a total of 174 636 vibronic basis states) is shown in Figure 8 (upper part). In our calculations there are two MLCT bands that tend to merge together to give the single band observed in the experiment. Indeed, the EA spectrum obtained by Boxer and co-workers clearly indicates the presence in the visible of at least two bands.[4] The computed bands are similar to those obtained for $(NH_3)_5$-Ru−bpy−$Ru(NH_3)_5^{5+}$; that is, one can be associated with the charge transfer from each metal atom to its nonadjacent pyr ring, and the other to the charge transfer from the metals to their adjacent rings.

In the EA spectrum (lower part of Figure 8) the two bands, due to their separation, which is overestimated, give a profile different in comparison with the experiments. While the highest energy part of the spectra is well reproduced, at lowest energy there is a sharp negative peak, which is absent in the experimental EA spectra where, after the positive lobe, there is a clear-cut diminution of the intensity but ΔA remains positive. Correspondingly, also the computed intensity of the central positive lobe (~2.5 eV) is remarkably overestimated. However, the first negative lobe might disappear when the inclusion of further degrees of freedom cause the complete merging of the two MLCT's in one single band.

Including only the site oscillators (vibronic coupling constants taken from ref 18), the energy and the intensity of the lowest energy band dramatically decrease (upper part of Figure 9) but the separation of the two bands increases. This separation cause, in the EA spectra (lower part of Figure 9), the appearance of a second derivative feature at ~1.5 eV, but the intensity of the peaks above 2 eV is in better agreement with the experimental results (1 order of magnitude less). For the $(NH_3)_5Ru-bpy-Ru(NH_3)_5^{4+}$ complex a simultaneous inclusion of bond and site

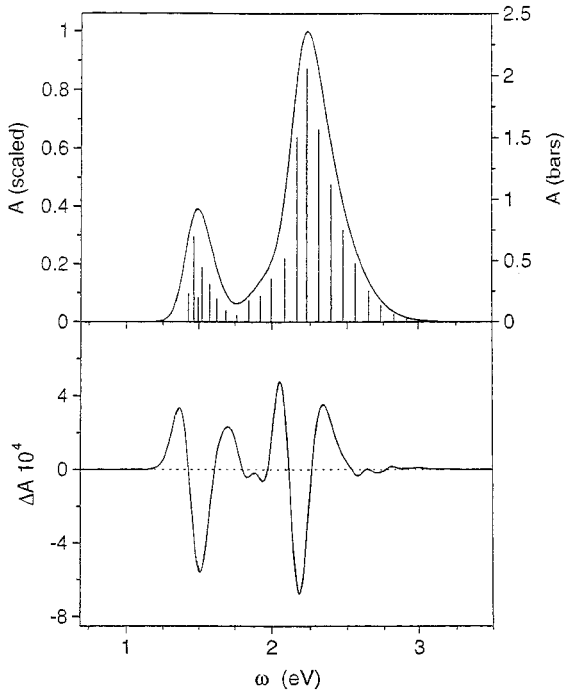

Figure 9. Absorption (upper part) and electroabsorption (lower part) spectrum of $[(NH_3)_5Ru-(4,4'\text{-bpy})-(NH_3)_5Ru]^{4+}$ as computed including only site oscillators.

oscillators seems thus necessary in order to verify if a reasonable agreement with the experimental results can be achieved.

It is important to underline that we have used here the same parameters for +5 and +4 complexes, and this choice, while avoiding a proliferation of parameters, unnecessary at this stage, may perhaps reveal a possible source of error.

Conclusions

In this article we have proposed and discussed a 4-site vibronic model Hamiltonian which can be useful for studying the near-IR−vis optical properties of partially localized compounds. This model is obtained by including site and bond vibrations and their coupling to the electronic motion in a 4-site electronic model previously presented,[21] and further discussed here.

An accurate study of the model, both within the adiabatic approximation and by exact methods, shows that the model indeed has the intrinsic signature of electron localization and it is therefore suitable for the study of compounds such as the 4,4′-bipyridine-bridged Ru dimer. Charge localization is seen by the presence of a double well in the adiabatic ground state, as well as by evidence of a localized wave function in exact calculations with slight asymmetric perturbation.

We have then computed the electroabsorption spectra of the complexes $(NH_3)_5Ru-bpy-Ru(NH_3)_5^{4+,5+}$. For mixed-valent (+5) dimer, the agreement with the experimental electroabsorption spectra is good in the entire low-energy region (up to the visible). For the +4 dimer (monovalent dimer), this agreement is less satisfactory but we think that could be substantially ameliorated by the contemporary inclusion of bond and site oscillators, which is computationally a hard task. However, these results appears to support our assignment of the ∼1 eV band to an MLCT transitions

The results presented here and the Raman resonance spectra of $(NH_3)_5Ru-bpy-Ru(NH_3)_5^{5+}$,[33] which only show features related to inter-ring stretching modes, represent a strong bias against the traditional assignment of the peak at ∼1 eV to an MMCT transition.

The MLCT transition at ∼2 eV corresponds mainly to the charge transfer from the metal to the nearest pyridine ring.

The two different MLCT transitions are also present in the +4 system. In the absorption spectra they should merge in a single band, but their presence is suggested by the EA spectra.

The model presented takes into account the bond (site−site) oscillators, whose involvement in the charge transfer transition has been shown by Raman resonance experiments. Our calculations confirm the importance of the Ru−ring stretching modes for a more reliable absorption line shape: this task is particularly important in the calculation of electroabsorption difference spectra, which is a small difference between two large quantities. Small errors in the determination of the absorption profile with or without the electric field may lead not only to a large error in the intensity of the difference spectra but also to an electroabsorption profile qualitatively wrong.

For $(NH_3)_5Ru-bpy-Ru(NH_3)_5^{5+}$, when bond oscillators are not included the relative intensity of the IR and visible features is remarkably different, in disagreement with the experimental results. These results underline also the importance of a correct evaluation of the vibronic coupling constant for the bond oscillators. For this purpose the results of the Raman resonance spectra seem to be more useful than crystallographic data. In fact, the latter can only show how the geometry of the ground state changes when an electron is subtracted to the whole system, while the former are able to give information on the dynamic dependence of the molecular vibrations from the electron transfer between different electronic states.

We have also presented arguments in favor of the thesis that a simultaneous inclusion of site and bond oscillators in the calculations may result in a better agreement between computed and experimental EA spectra.

Appendix

We examine here in more detail that in the past[21] what is the origin of the bands at ∼1 and ∼2 eV in the +5 ion, according to the Hamiltonian of eq 1. This is particularly relevant for the lowest energy transition since, as previously mentioned, our assignment (MLCT) is in contrast with the current interpretation (MMCT).

The exact computation requires the diagonalization of a 24 × 24 Hamiltonian matrix in the full CI space, but the final results can be easily interpreted at a semiquantitative level considering only the most relevant configurations involved.

Let us first consider the two mother configurations with three electrons on the metal sites (1 and 4; the bar is for the spin down): $|1, \bar{1}, 4\rangle$, $|4, 4, 1\rangle$. Promoting a single electron from a metal to the neighboring ring orbital, we generate two families of configurations. Taking only doublet states these are

$$|1\rangle = |1, \bar{1}, 4\rangle; \quad |2\rangle = \frac{1}{\sqrt{6}}(|1, \bar{2}, 4\rangle - 2|\bar{1}, 2, 4\rangle + |1, 2, \bar{4}\rangle);$$

$$|3\rangle = \frac{1}{\sqrt{2}}(|1, \bar{2}, 4\rangle - |1, 2, \bar{4}\rangle)$$

$$|1'\rangle = |4, \bar{4}, 1\rangle; \quad |2'\rangle = \frac{1}{\sqrt{6}}(|4, \bar{3}, 1\rangle - 2|\bar{4}, 3, 1\rangle + |4, 3, \bar{1}\rangle);$$

$$|3'\rangle = \frac{1}{\sqrt{2}}(4, \bar{3}, 1\rangle - |4, 3, \bar{1}\rangle)$$

Let us first ignore the coupling between pyr rings and consider

only one family, say the first. A little algebra leads to the following Hamiltonian and dipole matrices:

$$H = \begin{pmatrix} U & -3t/\sqrt{6} & t/\sqrt{2} \\ -3t/\sqrt{6} & \Delta & 0 \\ t/\sqrt{2} & 0 & \Delta \end{pmatrix}; \mu = \begin{pmatrix} -a & 0 & 0 \\ 0 & -b & 0 \\ 0 & 0 & -b \end{pmatrix} \quad \text{(A1)}$$

where a and b are respectively the Ru and pyr distance from the center of the molecule (in the middle of the bpy pyr−pyr single bond).

Due to the form of H one can easily verify that transforming to the new basis

$$|1\rangle, \quad \frac{\sqrt{3}}{2}|2\rangle - \frac{1}{2}|3\rangle, \quad \frac{1}{2}|2\rangle + \frac{\sqrt{3}}{2}|3\rangle \quad \text{(A2)}$$

it becomes block diagonal (the blocks have dimensions 2 and 1):

$$H_{22} = \begin{pmatrix} U & -t\sqrt{2} \\ -t\sqrt{2} & \Delta \end{pmatrix}; \quad H_{11} = \Delta \quad \text{(A3)}$$

The dipole matrix does not change.

The diagonalization of H_{22} gives rise to the ground state and to an excited state which is dipole connected with the ground. The energies are

$$E_g = \frac{U+\Delta}{2} - B, \quad E_e = \frac{U+\Delta}{2} + B; \quad B = \sqrt{\frac{(\Delta - U)^2}{4} + 2t^2} \quad \text{(A4)}$$

The other state is at energy Δ and is dark. We notice that taking $t = -0.73$, $U = 4.62$, and $\Delta = 5.06$, the bright transition is at about 2.1 eV (in satisfactory agreement with the experimental data for the MLCT in the Ru(II)−pyz ion) and the dark one is at about 1.3 eV. The next step consists of taking into account the ring−ring hopping term. For that purpose it is convenient first to build symmetric and antisymmetric combinations of pair of states of the two families. The main result of the introduction of the weak interaction between the two pyz rings is that (i) the dark transition borrows some oscillator strength (depending on the t' value) and contributes now to the spectrum (while the transition energies do not change very much); (ii) there appears a zero frequency transition due to the degeneracy (in this simplified picture) of the ground state in the symmetric and anti-symmetric manifolds. The complete diagonalization will remove this degeneration but the corresponding transition, which is then the real MMCT, is at very low frequency.

One may then conclude that, according to the four-site model, the 2 eV band correlates with the MLCT band present in Ru(II)−pyz monomer, while the 1 eV band is also an MLCT band originating from a dark state of the monomer which borrows oscillator strength from other transitions. This can be attributed to the ring−ring hopping term, i.e., to the activation of a charge-transfer interaction between the two moieties.

Acknowledgment. The authors express their gratitude to Prof. Mary Jo Ondrechen, Dr. Leonel F. Murga, and Dr. Ihsan A. Sheadi, from the Northeastern University of Boston, for helpful and fruitful discussions on the whole subject of Stark spectroscopy.

References and Notes

(1) Robin, M. B.; Day, P. *Adv. Inorg.Chem. Radiochem.* **1967**, *10*, 247.

(2) (a) Allen, G. C.; Hush, N. S. *Prog. Inorg. Chem.* **1967**, *8*, 357. (b) Hush, N. S. *Prog. Inorg. Chem.* **1967**, *8*, 391.

(3) Creutz, C.; Taube, H. *J. Am. Chem. Soc*. **1969**, *91*, 3988.

(4) (a) Oh, D. H.; Boxer, S. G. *J. Am. Chem. Soc.* **1990**, *112*, 8161. (b) Oh, D. H.; Sano, M.; Boxer, S. G. *J. Am. Chem. Soc.* **1991**, *113*, 6880.

(5) (a) Petrov, V.; Hupp, J. T.; Mottley, C.; Mann, L. C. *J. Am. Chem. Soc.* **1994**, *116*, 2171. (b) Lu, H.; Petrov, V.; Hupp, J. T. *Chem. Phys. Lett.* **1995**, *235*, 521.

(6) Hupp, J. T.; Dong, Y. *Inorg. Chem.* **1994**, *33*, 4421.

(7) Bencini, A.; Ciofini, I.; Daul, C. A.; Ferretti, A. *J. Am. Chem. Soc.* **1999**, *121*, 11418.

(8) (a) Creutz, C., *Prog. Inorg. Chem.* **1983**, *30*, 1. (b) Crutchley, R. J. *Adv. Inorg. Chem.* **1994**, *41*, 273. (c) Endicott, J. F.; Watzky M. A.; Song, X.; Buranda, T. *Coord. Chem. Rev.* **1994**, *41*, 273. (d) Watzky M. A.; Macatamgay, A. V.; Van Camp, R. A.; Mazzetto, S. E.; Song, X.; Endicott, J. F.; Buranda, T. *J. Phys. Chem.* **1997**, *101*, 8441.

(9) (a) Almaraz, A. E.; Gentil, L. A.; Baraldo, L. M.; Olabe. J, A. *Inorg. Chem.* **1996**, *35*, 7718. (b) Almaraz, A. E.; Gentil, L. A.; Baraldo, L. M.; Olabe. J, A. *Inorg. Chem.* **1997**, *36*, 1517. (c) Hornung, M. F.; Bauman, F.; Kaim, W.; Olabe, J. A.; Slep, L. D.; Fiedler, J. *Inorg. Chem.* **1998**, *37*, 311.

(10) (a) Rezvani, A. R.; Bensimon, C.; Cromp, B.; Reber, C.; Greedan, J. E.; Kondratiev, V. V.; Crutchley, R. J. *Inorg. Chem.* **1997**, *36*, 3322. (b) Nacklicki, M. L.; White, C. A.; Plante, L. L.; Evans, C. E. B.; Crutchley, R. J. *Inorg. Chem.* **1998**, *37*, 1880.

(11) Demadis, K. D.; Neyhart, G. A.; Kober, E. M.; White, P. S.; Meyer, T. J. *Inorg. Chem.* **1999**, *38*, 5948.

(12) (a) Macatamgay, A. V.; Mazzetto, S. E.; Endicott, J. F. *Inorg. Chem.* **1999**, *38*, 5091. (b) Macatamgay, A. V.; Endicott, J. F. *Inorg. Chem.* **2000**, *39*, 437.

(13) Piepho, S. B.; Krausz, E. R.; Schatz, P. N. *J. Am. Chem. Soc.* **1978**, *100*, 0, 2996.

(14) Zhang, L.-T.; Ko, J.; Ondrechen, M. J. *J. Am. Chem. Soc.* **1987**, *109*, 1666.

(15) Ondrechen, M. J.; Ko, J.; Zhang, L.-T. *J. Am. Chem. Soc.* **1987**, *109*, 1672.

(16) Piepho, S. B. *J. Am. Chem. Soc.* **1988**, *110*, 6319; **1990**, *112*, 4197.

(17) (a) Ferretti, A.; Lami, A. *Chem. Phys.* **1994**, *181*, 107. (b) Ferretti, A.; Lami, A. *Chem. Phys. Lett.* **1994**, *220*, 327.

(18) Ferretti, A.; Lami, A.; Ondrechen, M. J.; Villani, G. *J. Phys. Chem.*, **1995**, *99*, 10484; Erratum **1996**, *100*, 20174.

(19) Cave, R. J.; Newton, M. D. *Chem. Phys. Lett.* **1996**, *249*, 15.

(20) Reimers, J. R.; Hush, N. S. *Chem. Phys.* **1996**, *208*, 177.

(21) Ferretti, A.; Lami, A.; Villani, G. *Inorg. Chem.* **1998**, *37*, 2799; **1998**, *37*, 4460

(22) Von Kameke, A.; Tom, G. M.; Taube, H. *Inorg. Chem.* **1978**, *17*, 1790.

(23) (a) Murga, L. F.; Ferretti, A.; Lami, A.; Ondrechen, M. J.; Villani, G. *Inorg. Chem. Commun.* **1998**, *1*, 137. (b) Ferretti, A.; Lami, A.; Murga, L. F.; Shehadi, I. A.; Ondrechen, M. J.; Villani, G. *J. Am. Chem. Soc.* **1999**, *121*, 2594.

(24) Liptay, W. In *Excited States*; Lim, E. C., Ed.; Academic Press: New York, 1974; pp 129−229.

(25) Vance, F.; Williams, R. D.; Hupp, J. T. *Int. Rev. Phys. Chem.*, **1998**, *10*, 247.

(26) Bublitz, D.; Boxer, S. G. *Annu. Rev. Phys. Chem.* **1997**, *48*, 213.

(27) Shin, Y. K.; Brunschwig, B.; Creutz, C.; Sutin, N *J. Phys. Chem.* **1996**, *100*, 8157.

(28) Reimers, J. R.; Hush, N. S. *J. Phys. Chem.* **1991**, *95*, 9773. (b) Reimers, J. R.; Hush, N. S. In *Mixed Valence Systems: Applications in Chemistry, Physics and Biology*; Prassides, K., Ed.; Kluwer Academic Publishers: Dordrecht, 1991; pp 29−50

(29) Liptay, W. *Z. Naturforsch*. **1965**, *20A*, 272.

(30) Hubbard, J. *Proc. R. Soc. London* **1964**, *285*, 542.

(31) Wilson, E. B.; Decius, J. C.; Cross, P. C. *Molecular Vibrations*; McGraw-Hill: New York, 1955.

(32) Bozio, R.; Feis, A.; Zanon, I.; Pecile, C. *J. Chem. Phys.* **1989**, *91*, 13.

(33) Doorn, S. K.; Hupp, J. T.; Porterfield, D. R.; Campion, A.; Chase, D. B. *J. Am. Chem. Soc*. **1990**, *112*, 4999.

(34) Casswell, D. S.; Spiro, T. G. *Inorg. Chem.* **1987**, *26*, 18.

(35) Ould-Moussa, L.; Poizat, O.; Castellà-Ventura M.; Buntinx, G.; Kassab, E. *J. Phys. Chem.* **1996**, *100*, 2072.